A wavelet leaders-based climate classification of European surface air temperature signals

Adrien Deliège and Samuel Nicolay

University of Liège, Liège, Belgium

Abstract. We explain the wavelet leaders method, a tool to study the pointwise regularity of signals, which is closely related to some functional spaces. We use the associated multifractal formalism to show that surface air temperature signals are monofractal, i.e. these climate time series are regularly irregular. Then we use this result to establish a climate classification of weather stations in Europe which matches the Köppen-Geiger climate classification. This result could give rise to new criteria to determine the efficiency of current climatic models.

Keywords: Multifractal analysis, wavelet leaders method, climate time series analysis

1 Introduction

This work consists of a presentation of the wavelet leaders method (WLM) and its application to surface air temperature signals in Europe. The aim is to study the pointwise regularity of signals, which is defined as follows.

Definition 1. *Let $f : \mathbb{R} \to \mathbb{R}$ be a locally bounded function and x_0 a real number; f belongs to the Hölder space $C^\alpha(x_0)$ if there exist a polynomial $P_{x_0,\alpha}$ of degree at most α and a positive constant C such that the inequality*

$$|f(x) - P_{x_0,\alpha}(x)| \leq C|x - x_0|^\alpha$$

holds for all x in a neighbourhood of x_0. The uniform space $C^\alpha(\mathbb{R})$ is the space of functions satisfying the above inequality for all $x_0 \in \mathbb{R}$ with a uniform constant C.

A notion of regularity of f at x_0 is then given by the supremum of the exponents α such that f belongs to $C^\alpha(x_0)$, which is called the Hölder exponent of f at x_0 :

$$h_f(x_0) = \sup\{\alpha : f \in C^\alpha(x_0)\} \ .$$

If there exist two distinct real numbers with different Hölder exponents, then f is a multifractal function. On the other hand, if there exists $H > 0$ such that $h_f(x) = H$ for all $x \in \mathbb{R}$, then f is monofractal, which somehow means that f is "regularly irregular". For example, many space-filling functions ([11]), the well–known fractional Brownian motions ([20, 25]) and coded DNA sequences ([5]) display a monofractal behaviour.

Computing $h_f(x_0)$ is often difficult, if not impossible. One rather tries to get global information about the pointwise regularity of f. A global characterization is the spectrum of singularities of a function, defined as follows.

Definition 2. *The spectrum of singularities of a signal f is the function*

$$d_f : h \mapsto \dim\left(\{x \in \mathbb{R} : h_f(x) = h\}\right) \ ,$$

where $\dim(X)$ *is the Hausdorff dimension of the set X ([9]). In other words, $d_f(h)$ is the Hausdorff dimension of the set of points having h as Hölder exponent ([10]).*

Let us remark that a function is monofractal with Hölder exponent H if and only if the support of its spectrum of singularities is reduced to $\{H\}$.
In section 2, we define the notion of wavelet leader and we present the theorem that establishes the connection with pointwise regularity. A few multifractal formalisms have been developed to determine the spectrum of singularities of a signal (e.g. [10, 11, 22, 23]); among them is the wavelet leaders method introduced by Jaffard in [10], which is described in section 3. This formalism has already been successfully applied in several scientific fields, such as fully developed turbulence ([17]), heart rate variability ([2]), texture classification ([26]), and is used here in climatology. Eventually, in section 4, we apply this formalism to surface air temperature signals of some European weather stations. We first show that these signals are monofractal, then we establish a climate classification based on their Hölder exponent that matches the worldwide used Köppen–Geiger climate classification. We then proceed to a blind test to confirm the efficiency of this method before discussing the results.

2 Wavelet leaders and pointwise regularity

Definition 3. *We say that ψ is a wavelet with $n \in \mathbb{N}$ vanishing moments if $\psi \in \mathrm{L}^\infty(\mathbb{R})$, the function $x \mapsto x^k\psi(x)$ belongs to $\mathrm{L}^1(\mathbb{R})$ with $\int_{\mathbb{R}} x^k\psi(x)dx = 0$ for all $k \in \mathbb{N}$ such that $k < n$ and if $\hat{\psi}(0) = 0$ (where $\hat{\psi}$ denotes the Fourier transform of ψ).*

In addition, throughout this paper, we consider that the function ψ is compactly supported (see [6]) and n times continuously differentiable with $n > \alpha$, where α comes from theorem 1 below.

Proposition 1. *Under some general conditions ([6, 18]), it is possible to use a wavelet ψ to build an orthonormal basis of* $\mathrm{L}^2(\mathbb{R})$*. More precisely, if $f \in \mathrm{L}^2(\mathbb{R})$, then we have*

$$f(x) = \sum_{j,k\in\mathbb{Z}} c_{j,k}\psi(2^{-j}x - k) \ ,$$

where the wavelet coefficient $c_{j,k}$ is given by

$$c_{j,k} = 2^{-j}\int_{\mathbb{R}} f(x)\psi(2^{-j}x - k)dx \ .$$

If we denote by $\lambda_{j,k}$ the dyadic interval at the scale j and position k, i.e. $\lambda_{j,k} = [2^j k, 2^j(k+1))$, and by Λ the set of all dyadic intervals, then f can be written as follows:$f(x) = \sum_{\lambda \in \Lambda} c_\lambda \psi_\lambda$. In order to link the Hölder exponent of f at x_0 to the wavelet coefficients c_λ, we have to define the notion of wavelet leader.

Definition 4. *The wavelet leader associated to a dyadic interval λ is defined as*

$$d_\lambda = \sup_{\lambda' \subset \lambda} |c_{\lambda'}| \ ,$$

i.e. the supremum of the modulus of the wavelet coefficients associated to the dyadic intervals included in λ.

Let us remark that the wavelet leaders are bounded since the Cauchy–Schwarz inequality implies $|c_\lambda| \leq C \, \|f\|_{\mathrm{L}^2(\mathbb{R})} \, \|\psi\|_{\mathrm{L}^2(\mathbb{R})}$ for some positive constant C. We also need the following definition.

Definition 5. *The wavelet leader of x_0 at the scale j is defined as*

$$d_j(x_0) = \sup_{\lambda' \subset 3\lambda_{j,k}(x_0)} d_{\lambda'} \ ,$$

where $3\lambda_{j,k} = \lambda_{j,k-1} \cup \lambda_{j,k} \cup \lambda_{j,k+1} = [2^j(k-1), 2^j(k+2))$ and $\lambda_{j,k}(x_0)$ is the unique dyadic interval at the scale j containing x_0.

The link between pointwise regularity and the wavelet leaders is established in the following theorem.

Theorem 1. *1. If the bounded function f belongs to $C^\alpha(x_0)$, then there exist a positive constant C and an integer J such that*

$$d_j(x_0) \leq C 2^{\alpha j} \quad \forall j \leq -J \ . \tag{1}$$

2. Conversely, if there exist a positive constant C and an integer J such that inequality (1) is satisfied, and if there exists $\epsilon > 0$ such that f belongs to $C^\epsilon(\mathbb{R})$, then there exist a polynomial $P_{x_0,\alpha}$ of degree at most α and a positive constant C' such that the inequality

$$|f(x) - P_{x_0,\alpha}(x)| \leq C' |x - x_0|^\alpha \log |x - x_0| \tag{2}$$

holds for all x in a neighbourhood of x_0.

Proof. We define j_0 as

$$j_0 = \min\{j \in \mathbb{Z} : \mathrm{supp}(\psi) \subset B(0, 2^j) = (-2^j, 2^j)\} \ .$$

1. We set $k_0 = \max\{2, j_0 + 1\}$, j a negative integer and $\lambda' = \lambda_{j',k'} \subset 3\lambda_j(x_0)$, where $\lambda_j(x_0) = \lambda(j,k)$ for some $k \in \mathbb{Z}$. Let P be the polynomial such that

$f \in C^\alpha(x_0)$. Since the degree of P is strictly inferior to α, the hypothesis on the number of vanishing moments of ψ gives

$$|c_{\lambda'}| = \left| 2^{-j'} \int_{\mathbb{R}} (f(x) - P(x - x_0)) \psi(2^{-j'} x - k') dx \right| .$$

Since $\text{supp}(\psi) \subset B(0, 2^{j_0})$ and $B(2^{j'}k', 2^{j_0+j'}) \subset B(x_0, 2^{k_0+j})$, we have

$$\begin{aligned} |c_{\lambda'}| &\leq 2^{-j'} \int_{B(2^{j'}k', 2^{j_0+j'})} |f(x) - P(x - x_0)||\psi(2^{-j'} x - k')| dx \\ &\leq 2^{-j'} \int_{B(x_0, 2^{k_0+j})} |f(x) - P(x - x_0)||\psi(2^{-j'} x - k')| dx . \end{aligned}$$

Since $f \in C^\alpha(x_0)$, there exist $C > 0$ and $K \in \mathbb{N}$ such that, for all $j \leq -K$, the inequality $|f(x) - P(x - x_0)| \leq C 2^{j\alpha}$ holds for all x such that $|x - x_0| \leq 2^j$. In particular, if $j \leq -K - k_0 = -J$, we get

$$|c_{\lambda'}| \leq C 2^{(k_0+j)\alpha} \int_{\mathbb{R}} 2^{-j'} |\psi(2^{-j'} y + 2^{-j'} x_0 - k')| dy \leq C_0 2^{j\alpha} .$$

2. In this part of the proof, the notation C refers to positive constants and thus may have different values at each occurrence of C. Also, let us note two general remarks used below, which we will refer as Remark(1) and Remark(2):

1. Given $R, x \in \mathbb{R}$ and $j, k \in \mathbb{N}$ such that $R > 2^j$ and $2^j k \in B(x, R)$, we have $\lambda_{j,k} \subset B(x, 2R)$.
2. Given a dyadic interval $\lambda = \lambda_{j,k}$ and $x \in \mathbb{R}$ such that $\lambda \subset B(x, 2^j)$, then there exists $k' \in \mathbb{Z}$ such that

$$\lambda \subset B(x, 2^j) \subset \lambda_{j+1,k'} \cup \lambda_{j+1,k'+1} .$$

Also, if $x_0 \in B(x, 2^j)$, then $|c_\lambda| \leq d_{j+1}(x_0)$.

As shown in [16], it is enough to prove that there exist a positive constant C' and a positive integer J' such that, for every $j \leq -J'$, there exists a polynomial P_j of degree strictly inferior to α such that

$$\sup_{|x - x_0| \leq 2^j} |f(x) - P_j(x - x_0)| \leq C' 2^{j\alpha} |\log(2^{\alpha j})| .$$

Moreover, as shown in [6, 18], every function $f \in \mathrm{L}^2(\mathbb{R})$ can be decomposed as $f(x) = \sum_{j'=-\infty}^{1} f_{j'}(x)$, where $f_{j'} = \sum_k c_{j',k} \psi_{j',k} = \sum_\lambda c_\lambda \psi_\lambda$ if $j' \leq 0$, and $f_1 = \sum_k c_k \varphi(. - k)$, where φ is a compactly supported wavelet arbitrarily smooth. We consider $j \leq -J'$ with $J' = J + 2 + j_0$, and we set $m = \lfloor \alpha \rfloor$ if $\alpha \notin \mathbb{N}$, $m = \alpha - 1$ if $\alpha \in \mathbb{N}$, and we define the polynomial P_j as

$$P_j(x) = \sum_{j'=j}^{1} \sum_{n=0}^{m} \frac{x^n}{n!} D^n f_{j'}(x_0) ,$$

which has degree at most $m < \alpha$. Then we get

$$|f(x) - P_j(x - x_0)| \leq \underbrace{\sum_{j'=-\infty}^{j-1} |f_{j'}(x)|}_{(1)} + \underbrace{\sum_{j'=j}^{1} \left| f_{j'}(x) - \sum_{n=0}^{m} \frac{(x-x_0)^n}{n!} D^n f_{j'}(x_0) \right|}_{(2)} .$$

Let us examine relation (2), for $x \in B(x_0, 2^j)$. Taylor's formula gives

$$\left| f_{j'}(x) - \sum_{n=0}^{m} \frac{(x-x_0)^n}{n!} D^n f_{j'}(x_0) \right| \leq C 2^{j(m+1)} \sup_{x \in B(x_0, 2^j)} |D^{m+1} f_{j'}(x)| .$$

Also, for $j' \leq 0$, we have

$$|D^{m+1} f_{j'}(x)| \leq 2^{-j'(m+1)} \sum_{\substack{k \text{ s.t.} \\ 2^{j'}k \in B(x, 2^{j_0+j'})}} |c_\lambda| |(D^{m+1}\psi)(2^{-j'}x - k)| .$$

Considering Remarks (1) and (2), every coefficient $|c_\lambda|$ is bounded by $d_{2+j_0+j'}(x_0)$, and therefore $|c_\lambda| \leq C 2^{\alpha j'}$ (by hypothesis if $j' \leq -J'$, by Cauchy-Schwarz inequality else). Moreover, $|D^{m+1}\psi|$ is bounded (see definition 3), and the number of integers k such that $2^{j'}k \in B(x, 2^{j_0+j'})$ is at most 2^{j_0+1}, so if $j' \leq 0$, $|D^{m+1} f_{j'}| \leq C 2^{-j'(m+1)} 2^{\alpha j'}$ for some constant C. If we assume that the wavelet φ is smooth enough, there exists a constant C such that $\left|D^{m+1} f_1\right| \leq C 2^{-j(m+1-\alpha)}$. Therefore, (2) is bounded as follows:

$$\begin{aligned}(2) &\leq C 2^{j(m+1)} \left(C 2^{-j(m+1-\alpha)} + C \sum_{j'=j}^{0} (2^{m+1-\alpha})^{-j'} \right) \\ &\leq C 2^{j(m+1)} \left(C 2^{-j(m+1-\alpha)} + C 2^{-j(m+1-\alpha)} \right) \leq C 2^{j\alpha} \leq C 2^{j\alpha} |\log(2^{j\alpha})| .\end{aligned}$$

Let us examine (1). Let $J_1 \in \mathbb{N}$ be such that $2^{-\epsilon J_1} \leq 2^{j\alpha} < 2^{-\epsilon(J_1-1)}$. Then

$$(1) = \sum_{j'=-\infty}^{j-1} |f_{j'}(x)| \leq \underbrace{\sum_{j'=-\infty}^{-J_1} |f_{j'}(x)|}_{(3)} + \underbrace{\sum_{j'=-J_1+1}^{j-1} |f_{j'}(x)|}_{(4)} .$$

Using the result of Jaffard ([10],[21]) stating that, if $f \in C^\epsilon(\mathbb{R})$, then there exists a constant C such that $||f_{j'}||_{L^\infty(\mathbb{R})} \leq C 2^{\epsilon j'}$, then (3) is bounded as follows:

$$(3) \leq C \sum_{j'=-\infty}^{-J_1} 2^{\epsilon j'} = C \frac{2^{-\epsilon J_1}}{1 - 2^{-\epsilon}} \leq C 2^{j\alpha} \leq C 2^{j\alpha} |\log(2^{j\alpha})| .$$

We now consider relation (4). Let j' be such that $-J_1 + 1 \leq j' \leq j - 1$. We have

$$|f_{j'}(x)| \leq \sum_{\substack{k \text{ s.t.} \\ 2^{j'}k \in B(x, 2^{j_0+j'})}} |c_\lambda| |\psi_\lambda(x)| ,$$

and every λ in this sum is included in $B(x, 2^{1+j_0+j'})$ (by Remark(1)). Therefore, Remark(2) implies that every λ is taken into account when computing either $d_{2+j}(x_0)$ (if $j' + j_0 + 1 \leq j$) or $d_{3+j'}(x_0)$ (else), and both cases lead to $|c_\lambda| \leq C2^{\alpha j}$. Again, $|\psi_\lambda|$ is bounded thus $|f_{j'}| \leq C2^{j\alpha}$ for some constant C. Hence, the following inequalities arise:

$$(4) \leq C2^{\alpha j} \sum_{j'=-J_1+1}^{j-1} 1 = C2^{\alpha j}(J_1 + j - 1) \leq C2^{\alpha j}(J_1 - 1) \leq C2^{\alpha j} |\log(2^{\alpha j})| \ ,$$

where the last inequality comes from the definition of J_1, which ends the proof.

Theorem 1 gives the following corollary.

Corollary 1. *The Hölder exponent of f at x_0 is given by*

$$h_f(x_0) = \liminf_{j \to -\infty} \frac{\log d_j(x_0)}{\log 2^j} \ .$$

3 Wavelet leaders–based multifractal formalism

Corollary 1 is rarely used in practice since it is hard or meaningless to compute the Hölder exponent of f at every point. As mentioned, one rather uses other mathematical tools to have a global characterization of the regularity of a signal. We present here the wavelet leaders method introduced by Jaffard in [10], which gives the spectrum of singularities of a function.

First, for every scale j, we define

$$S(q, j) = 2^j \sum_{\lambda \in \Lambda_j} d_\lambda^q \ ,$$

where the sum is taken over the dyadic intervals λ for which $d_\lambda \neq 0$, Λ_j being the set of dyadic intervals at scale j and q being a real parameter.

Then we set the function w as

$$w(q) = \liminf_{j \to -\infty} \frac{\log(S(q, j))}{\log 2^j} \ , \tag{3}$$

which can be numerically obtained using a $\log - \log$ regression. The spectrum of singularities associated to this method defined as

$$d_f^w(h) = \inf_q \{qh - w(q)\} + 1 \ . \tag{4}$$

Let us give the heuristic arguments underpinning this method. Equation (3) gives the asymptotic behaviour of the sum $\sum_{\lambda \in \Lambda_j} d_\lambda^q$ (as $j \to -\infty$):

$$\sum_{\lambda \in \Lambda_j} d_\lambda^q \sim 2^{(w(q)-1)j} \ . \tag{5}$$

On the other hand, the number of dyadic intervals at the scale j containing a point of Hölder exponent h should be about $2^{-d(h)j}$, and for these intervals, theorem 1 gives $d_\lambda^q \sim 2^{hqj}$. Thus the global behaviour of the sum should be about $2^{(hq-d(h))j}$ where the exponent is as large as possible. Since $j < 0$, we have

$$\sum_{\lambda \in \Lambda_j} d_\lambda^q \sim 2^{\inf_h \{hq-d(h)\}j} \ . \tag{6}$$

Comparing relations (5) and (6) gives

$$\sup_h \{d(h) - hq\} = 1 - w(q) \ ,$$

and an inverse Legendre transform gives the expected relation (4), provided that w and d are concave functions. In practice one can thus hope to have $d_f = d_f^w$. For theoretical results about the relations between d_f and d_f^w, see [10].
Let us remark that if w is a straight line with slope H, then the support of the spectrum of singularities is reduced to $\{H\}$ and therefore the signal f is monofractal with exponent H. In this case, we define a norm in the uniform Hölder space $C^H(\mathbb{R})$ as

$$\|f\|_{C^H} = \sup_{j,k} \{|c_{j,k}|/2^{jH}\} := N \ ,$$

where the coefficients $(c_{j,k})_{j,k\in\mathbb{Z}}$ are the wavelet coefficients of f.

4 Surface air temperature analysis

4.1 Data description and results

We performed the wavelet leaders method described above to analyze the regularity of surface air temperature signals collected from the European Climate Assessment and Dataset ([1]). These consist of daily mean temperatures between the years 1951 and 2003 of weather stations spread across Europe. We edged the area of interest to parallels 36°N (includes Spain, Italy, Greece) and 55°N (Ireland, Germany) and meridians 10°W (Ireland, Portugal) and 40°E (Ukraine) to have a consistent geographic zone and limit the effects of latitude. We selected weather stations for which the daily mean temperatures were calculated as average of maximum and minimum daily mean temperatures. Also, only weather stations located below 1000 meters of altitude were kept in order to prevent altitude from interfering in the analysis. We found 115 weather stations satisfying these criteria (see Fig. 1).

First, the signals are checked, in the sense that temperatures exceeding 50°C or going down −60°C are considered as suspicious and are therefore removed from the signal. Missing data do not affect the regularity of the signals since most of them (97 out of 115) display less than 1% of missing data and for the others, this percentage is at most 7% (with only 5 stations beyond 4%). Also, in order to get more stable and accurate numerical results, we consider the

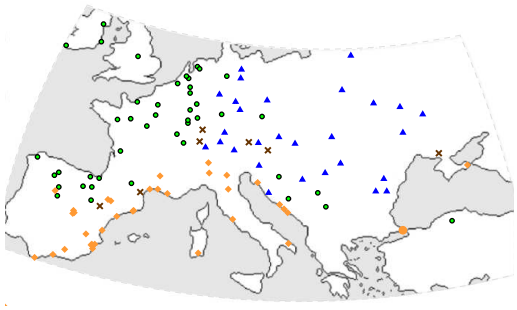

Fig. 1. The 115 selected weather stations. Stations were classified according to the Köppen–Geiger system (see text): green discs correspond to Oceanic stations (Cb-type), blue triangles correspond to continental stations (D-type), orange diamonds correspond to Mediterranean stations (Ca-type) and brown crosses correspond to stations whose climates were erroneously predicted.

temperature profiles instead of the original signals, i.e. the n^{th} value of a signal is replaced by the sum of its first n values.

A first result is the linear behaviour of the functions w associated to the signals, as shown in Fig. 2, for which the mean coefficient of determination is equal to $R^2 = 0.9975 \pm 0.0028$. This implies that the surface air temperatures are monofractal and their regularity can then be obtained as the slope of these functions. The Hölder exponents range from 1.093 to 1.43 and the norms from 8.23 to 30.45, as illustrated in Fig. 3.

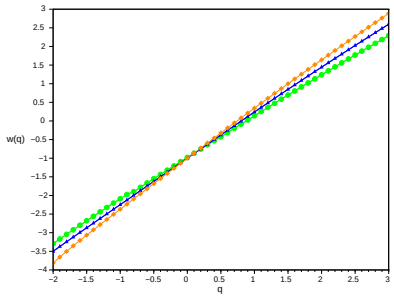

Fig. 2. The function w associated to the surface air temperature of several weather stations. In green,the city of Aachen (50°46′N, 6°06′E, Cb-type), in blue the town of Shepetivka (50°10′12″N, 27°03′E, Db-type) and in orange the city of Milano (45°28′18″N, 9°11′21″E, Ca-type). The remarkably linear behaviour of w means that temperatures data are monofractal. The slope of w gives the Hölder exponent; here we obtain $H = 1.156$ for Aachen, $H = 1.218$ for Shepetivka and $H = 1.358$ for Milano.

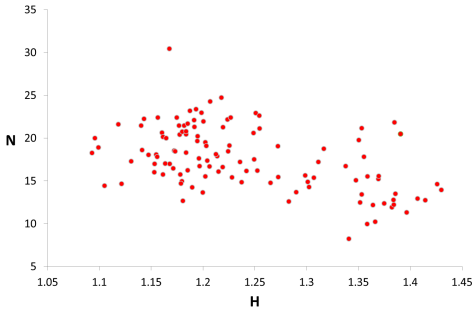

Fig. 3. Distribution of the Hölder exponents and norms of the signals.

The monofractal nature of such signals is not so surprising since some previous studies show the existence of long range correlations in the noise of such signals ([7, 15]). However, let us remark that the detrended fluctuation analysis used in [15] can not be applied to the raw data as it is done here ([5, 7]): in our work we keep information about the seasonal variation. Let us also note that other methods such as the wavelet transform modulus maxima and the S^ν-based method ([13]) also lead to the same conclusions.

4.2 Relation with climate types

The next natural step is to investigate the possible connections between the regularity of the signals and the climate type the stations are associated to. The climate classification used as reference is the celebrated Köppen–Geiger climate classification described in [14, 24], which is still largely used ([12, 19, 27]). It is based on maximum and minimum monthly mean temperatures and on precipitation, but since we limit our study to temperature signals, we do not take precipitation into account, which leads to a slight simplification of the classification. As shown in Fig 4, the 115 weather stations are divided in four different types of climate: Mediterranean (Ca), Oceanic (Cb), hot summer continental (Da) and continental temperate (Db). Since Da–type climate is rare in Europe (it is met only near the Black Sea), categories Da and Db are merged to form the continental climate type (D). Also, stations close to 0.5°C of another type of climate are also associated to this second category. This is due to the fact that for some of them (12.2%) the type of climate has changed during the years. With these considerations, the analyzed data set is made up of 33% of Cb–type stations, 30% of Ca–type, 21% of D–type, 9% of Cb and D–type and 7% of Cb and Ca–type.

In order to check if the regularity of the signals is related to the type of climate the stations are associated to, every point of Fig 3 is colored according to its type of climate, as illustrated in Fig. 5. One can clearly see that stations with the same climate are located in the same area of the plane. This gives us the possibility to divide it into rectangles such that each of them is associated

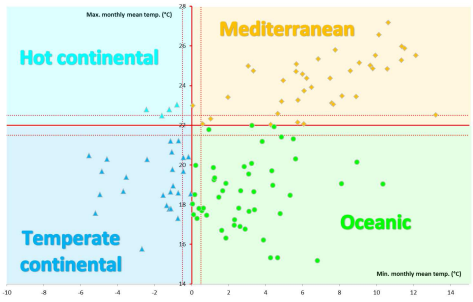

Fig. 4. Distribution of the weather stations within the different climate types in Europe.

to a type of climate and such that the underlying rectangle-based classification matches Köppen's for most of the stations (see Fig. 5). If the set of vertices of the rectangles is $\{(x, y) : x \in \{0, H_1, H_2\}, y \in \{0, N_1, N_2\}\}$, then optimal results occur when the values of the parameters H_1, H_2, N_1, and N_2 (see Fig. 5) are respectively $H_1 = 1.186$, $H_2 = 1.275$, $N_1 = 14.81$ and $N_2 = 16.18$, in which case 93.9% of the stations are correctly associated to their climate type (see Fig. 1 and Fig. 5). Obviously norms do not have an important impact on the multifractal–based classification, and without taking this parameter into account, 89.6% of the stations are still correctly classified.

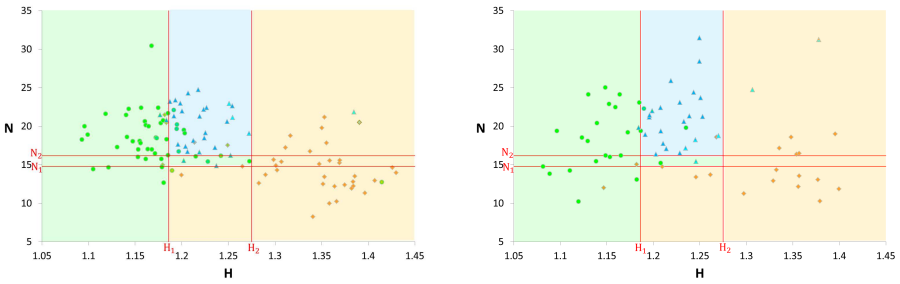

Fig. 5. The cut-out of the right upper quarter–plane defined by the Hölder exponent (abscissa) and the norm (ordinate) induced by the Köppen–Geiger classification. The left panel displays the points corresponding to the 115 reference stations, the right one shows the 69 other stations used for the blind test (see text). One can see that in both cases, points of the same color (Green: Cb, Orange: Ca, Blue: Db, Cyan: Da) are concentrated in the same rectangles.

In order to confirm these results and to validate the method used in this work, we performed a blind test, i.e. we selected 69 other weather stations spread across Europe and analyzed their regularity using the wavelet leaders method. To do

so, we allow shorter time series (we require at least 40 years of data between 1951 and 2003) and we admit signals for which daily mean temperatures are computed in a different way. Leaving unchanged the values of H_1, H_2, N_1, N_2, the multifractal–based classification matches Köppen's for 88.4% of the stations, and without the norm, 84.1% are still correctly classified (see Fig. 5).

4.3 Conclusions

The wavelet leaders method allows us to show that surface air temperature signals are monofractal and that their belonging to functional spaces reflects their temperature-based Köppen-Geiger climate type. Oceanic stations display the lowest Hölder exponents, while the Mediterranean ones have the largest and continental climate type has intermediate exponents. This implies that, on a daily basis, Oceanic climate is more irregular, less stable than the two others. On the other hand, Mediterranean stations have more stable and maybe predictable climate. The natural explanation ([7, 8]) comes from the North Atlantic Oscillation (NAO), which is a difference of pressure between the Azores and Iceland that induces winds and air streams mostly on the Western part of Europe. It thus have a larger impact on Oceanic regions. Conversely, the South part of Europe is more subject to anticyclonic conditions which induce much more stability and regularity in temperature signals.

This work gives satisfying results for Europe, but future work could consist of an extension of this method to other continents or global temperatures. Other climate indices such as pressure or precipitation could also be analyzed. Finally, this multifractal–based classification could help to check the validity of current climatic models, by comparing the regularity of original signals to the regularity of signals predicted by these models.

References

1. European Climate Assessment and Dataset, `http://eca.knmi.nl`
2. Abry, P., Wendt, H., Jaffard, S., Helgason, H., Goncalves, P., Pereira, E., Charib, C., Gaucherand, P., Doret, M.: Methodology for multifractal analysis of heart rate variability: From LF/HF ratio to wavelet leaders. Nonlinear Dynamic Analysis of Biomedical Signals EMBC conference (IEEE Engineering in Medicine and Biology Conferences) (2010).
3. Arneodo, A., Audit, B., Bacry, E., Manneville, S., Muzy, J.F., Roux, S.G.: Thermodynamics of fractal signals based on wavelet analysis: application to fully developed turbulence data and DNA sequences. Physica A 254, 24–45 (1998)
4. Arneodo, A., Audit, B., Decoster, N., Muzy, J.F., Vaillant, C.: The science of Disasters, 26–102, Springer (2002)
5. Arneodo, A., Bacry, E., Graves, P.V., Muzy, J.F.: Characterizing Long-Range Correlations in DNA Sequences from Wavelet Analysis. Phys. Rev. Lett. 74, 3293–3296 (1995)
6. Daubechies, I.: Ten Lectures on Wavelets. SIAM (1992)
7. Deliège, A., Nicolay S.: Monofractal nature of air temperature signals reveals their climate variability. Submitted for publication.

8. Deliège, A., Nicolay S.: Koppen–Geiger classification recovered via air temperature wavelet analysis. Submitted for publication.
9. Falconer, K.: The Geometry of Fractal Sets. Cambridge Tracts in Mathematics, Cambridge University Press (1986)
10. Jaffard, S.: Wavelet techniques in multifractal analysis. Proceedings of symposia in pure mathematics 72, 91–152 (2004)
11. Jaffard, S., Nicolay, S.: Pointwise smoothness of space-filling functions. Appl. Comput. Harmon. Anal. 26, 181–199 (2009)
12. Jylhä, K., Tuomenvirta, H., Ruosteenoja, K., Niemi-Hugaerts, H., Keisu, K., Karhu, J.: Observed and Projected Future Shifts of Climatic Zones in Europe and Their Use to Visualize Climate Change Information. Wea. Clim. Soc. 2, 148–167 (2010)
13. Kleyntssens, T., Esser, C., Nicolay, S.: A multifractal formalism based on the S^ν spaces: From theory to practice. Submitted for publication.
14. Köppen, W., Geiger, R.: Handbuch der Klimatologie, 1–44, Borntraeger (1936)
15. Koscielny-Bunde, E., Bunde, A., Havlin, S., Roman, H. E., Goldreich, Y., Schellnhuber, H.–J.: Indication of a Universal Persistence Law Governing Atmospheric Variability. Phys. Rev. Lett. 81, 729–732 (1998)
16. Kreit, D., Nicolay, S.: Generalized Hölder spaces. Submitted for publication.
17. Lashermes, B., Roux, S.G., Abry, P., Jaffard, S.: Comprehensive multifractal analysis of turbulent velocity using wavelet leaders. Eur. Phys. J. B. 61 (2), 201–215 (2008)
18. Mallat, S.: A Wavelet Tour of Signal Processing. Academic Press (2008)
19. Manabe, S., Holloway, J.L.: The seasonal variation of the hydrologic cycle as simulated by a global model of the atmosphere. J. Geophys. Res. 80, 1617–1649 (1975)
20. Mandelbrot, B., Van Ness, J.: Fractional Brownian motions, fractional noises and applications. SIAM Review 10, 422–437 (1968)
21. Meyer, Y.: Ondelettes et Opérateurs I: Ondelettes. Hermann, Paris (1990)
22. Muzy, J.F., Bacry, E., Arneodo, A.: Wavelets and multifractal formalism for singular signals: Application to turbulence data. Phys. Rev. Lett. 67, 3515–3518 (1991)
23. Parisi, G., Frisch, U.: Fully developed turbulence and intermittency. In Turbulence and Predictability in Geophysical Fluid Dynamics and Climate Dynamics, Proc. of Int. School, 84–88 (1985)
24. Peel, M., Finlayson, B., McMahon, T.: Updated world map of the Koppen-Geiger climate classification. Hydrol. Earth Syst. Sci. 11, 1633–1644 (2007)
25. Taqqu, M., Eberlain, E.: Dependence in Probability and Statistics, 137–165, Birkhäuser, Boston (1985)
26. Wendt, H., Abry, P., Jaffard, S., Ji, H., Shen, Z.: Wavelet leader multifractal analysis for texture classification. Proc IEEE conf. ICIP 2009, 3829–3832 (2009)
27. Zhou, L., Dickinson, R., Dai, A., Dirmeyer, P.: Detection and attribution of anthropogenic forcing to diurnal temperature range changes from 1950 to 1999: comparing multi-model simulations with observations. Clim. Dyn. 35, 1289–1307 (2010)